5-13-2021

Enhancement of Anti-tumor Efficacy of an Armed Oncolytic Virus: VSV-SKPC

Breona Luker
bluker2@student.gsu.edu

Enhancement of Anti-tumor Efficacy of an Armed Oncolytic Virus: VSV-S_{KPC}

by

Breona T. Luker

Under the Direction of Ming Luo , PhD

A Thesis Submitted in Partial Fulfillment of the Requirements for the Degree of

Master of Science

in the College of Arts and Sciences

Georgia State University

2021

ABSTRACT

Immunotherapy for treatment of pancreatic ductal adenocarcinoma (PDAC) continues to be an area of focus in the field of oncology. PDAC remains mostly incurable. The newest pillar of cancer treatments, immunotherapy, provides promises to patients as a viable option. However, the immunosuppressive microenvironment of PDAC tumors is one of the limitations on treatment efficacy. Thus, it was strategized that reactivation of the tumor's suppressive microenvironment could lead to an increased efficacy of treatment. The use of an armed oncolytic virus (OV) to infect the tumor has shown a potential to alter the tumor microenvironment (TME) more effectively in comparison with its wildtype counterpart. Vesicular stomatitis virus (VSV) was engineered to express Smac, (VSV-S), a protein found in the intrinsic pathway of apoptosis. The ability of Smac to interact with the inhibitor of apoptosis proteins (IAPs) makes VSV-S more effective in killing cancer cells. In addition, it was determined that adapting the virus to the cell line by limited dilution increased VSV-S to selectively target the murine cancer cell, KPC. Using a C57BL/6 mice model, subcutaneous implanted KPC tumors were intratumorally injected with VSV-S_{KPC}. After the infection by VSV-S, tumor size was greatly reduced and the survival rate was greatly increased. In the infected tumors, neutrophils were significantly increased, whereas macrophages were largely reduced, especially immunosuppressive M2-macrophages. The overall TME was also more immunologically active, which is proven by the reduced levels of cytokines and biomarkers including TGF-β, Arginase -1 and IL-10. This study indicates that the treatment of VSV-S was successful in the reactivation of the immunosuppressive TME and inhibition of tumor growth.

INDEX WORDS: pancreatic cancer, apoptosis, VSV-S, macrophages, cytokines, microenvironment

Enhancement of Anti-tumor Efficacy of an Armed Oncolytic Virus: VSV-S_{KPC}

by

Breona T. Luker

Committee Chair: Ming Luo

Committee: Jenny Yang

Gregory Poon

Electronic Version Approved:

Office of Graduate Services

College of Arts and Sciences

Georgia State University

May 2021

DEDICATION

To my daughter, Hunter Rose.

ACKNOWLEDGEMENTS

I would like to sincerely thank Dr. Ming Luo for your mentorship. I would also like to thank undergraduate students, Channen Mickler and Bhavana Suresh, working alongside you has been a great learning opportunity. To the current and former graduate students in our 5th floor lab, Andrew Brown, Shelby Mcmanus, James Ross Terrell, Chelsea Severin, and Sijia Tang, thank you for your continued support. To the other contributing labs at Georgia State University, Emory University and the University of South Carolina School of Medicine thank you for your contributing efforts towards this project. Finally, I would like to thank Drs. Kensei Komatsu and Jian-Dong Li for their help in luciferase imaging.

TABLE OF CONTENTS

LIST OF FIGURES

LIST OF TABLES

LIST OF ABBREVIATIONS

VSV-S: Vestibular stomatitis virus-SMAC

PD-L1: Programmed Death Ligand-1

SMAC: SMAC Mimetics

IAP: Inhibitor Apoptosis Proteins

TNF: Tumor Necrosis Factor

TME: Tumor Microenvironment

PC: Pancreatic Cancer

MHC: Major histocompatibility complex

IHC: Immunohistochemistry

OV: Oncolytic Virus

TAM: Tumor associated macrophages

PFU: Plaque forming unit

PDAC: Pancreatic Ductal Adenocarcinoma

IL-10: Interleukin-10

TGF-β: Transforming Growth Factor-Beta

CAF: Cancer-associated fibroblast

ECM: Extracellular matrix

1 INTRODUCTION

1.1 Pancreatic Ductal Adenocarcinoma (PDAC) Background Significance

Pancreatic Ductal Adenocarcinoma (PDAC) has an average 5-year survival rate of less than 10%; surgery is the only possible cure for the disease but the time of diagnosis is key for successful results. For most patients, surgical removal of the tumor is not possible because the early stages of the disease can easily be missed on a CT scan. This is due to the similar attenuation between the diseased pancreas and a healthy pancreas. Approximately 30% of patients with the disease present at late stages where the tumor has begun to metastasize. Aside from the late stage diagnosis with PDAC, the disease is also lethal because of aggressive growth and therapy resistance [1]. Moreover, other treatments such as chemotherapy have shown median overall survival rates for late-term PDAC.

Combination of 5-fluoruracil (5-FU), leucovorin (LV), irinotecan, and oxaliplatin (FOLFIRINOX) and gemcitabine-nab-paclitaxel has improved survival for patients with early stages of the disease. However, a significant amount of trials with other combination therapies, with the addition of drugs targeting new pathways, have yet to improvement cancer treatment. Recently, novel immunotherapies have provided promising results in solid tumors such as melanoma and renal cell carcinoma. Clinical success is due to the immune checkpoint inhibitors and adoptive cell therapy activity in these cancer types. This new pillar of cancer treatment is widely used to combat several types of diseases but immunotherapy-based treatment in PDAC has yet to prove valuable. In clinical trials of anti-PD-L1 and anti-CTLA-4 antibodies, positive responses were infrequent. This type of cancer has an immune-suppressive and therapy-resistant microenvironment. To overcome these challenges, reactivation of the immunosuppressive tumor microenvironment (TME) is an important approach [2].

1.2 The Tumor Microenvironment of PDAC

PDAC is far less accessible by immunotherapy for a multitude of reasons. One is the stromal desmoplastic reaction where the cancer invasion induces new matrix formation by activation of stromal cells. The invasion of epithelial tumor cells into the underlying connective tissue stroma causes dynamic changes to its microenvironment (Figure 1.1). The reaction causes negative regulation in immune responses and the immune suppressive tumor microenvironment (TME) suppresses antitumor T cells with the infiltration of myeloid derived suppressive cells and Treg cells. Activated antitumor T cells are also eliminated by PDAC directly in a process known as “immune privilege” [3].

1.2.1 The Role of Immune Checkpoint Inhibitors

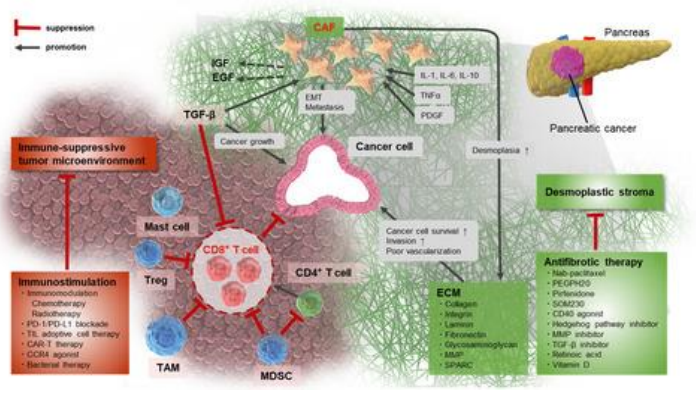

Figure 1.1: Suppressive and promotional components in the TME of Pancreatic cancer

The TME is a complex meshwork of extracellular matrix (ECM) macromolecules that are filled with a collection of cells like cancer-associated fibroblasts (CAFs) [4]. Its presence in the desmoplastic stroma in PDAC promote tumor growth, cell invasion and metastasis. The immunosuppressive Treg cell, myeloid- derived suppressor cells and tumor-associated macrophages (TAM) suppress the $CD8^+$ T cells (Figure 1.1). Transforming growth factor- β (TGF-β), a highly pleiotropic cytokine, suppresses the T cell and promotes tumor growth. Cytokine interleukin-10 (IL-10) promotes the CAFs that are responsible for metastasis, a

prominent challenge in PDAC diagnosis. More devastatingly, an overexpression of arginase is a poor prognostic factor in a wide variety of cancers, specifically PDAC. Since myeloid cells are major contributors to immune defense against pathogens and play a role in tissue remodeling, cells associated with strong immunosuppressive functions have been termed myeloid-derived suppressor cells (MDSCs). These cells express high levels of arginase which, plays an opposite role in immune response and is one of the main mechanism of immunosuppression. A reduction in these levels has the potential to make the TME more immunologically active.

Anti-PD-1/PD-L1, immunotherapy treatments for advanced melanomas aim to block a pathway that shields tumor cells from immune responses. Anti PD-1 is an immune checkpoint inhibitor that activates tumor specific CD^+ T cell responses. The antibody provides a new path for therapy with emerging potential. The utilization of the antibodies have shown promising results in clinical treatments. It also shows a correlation between the burden of tumor mutation and $CD8^+$ T cells with PD-1 and PD-L1 expression levels in the TME.

$CD8^+$ T cells are a critical subpopulation of major histocompatibility complex class I (MHC) restricted T cells and help mediate adaptive immunity [3]. Low expression of MHC-I molecules makes it difficult to mark infected cells since foreign antigens present on the complex. The lack of T cell immunity is the main reason the immune checkpoint blockade is therapeutically ineffective in PDAC. Additionally, a reactionary immune response is a result of the tumor antigenic strength. Hence, immunogenicity prediction by neoantigen quality metrics shows a correlation to the survival of patients with the disease. To account for these challenging conditions, a combination of chemotherapy or radiation with immunotherapy are in clinical trial stages to determine viability.[4].

Currently, a new therapy has been introduced as an option to improve the efficacy of immunotherapy. Especially in combination with other successful treatments. The efficacy of anti-PD-1 treatment was drastically enhanced with the combination of a oncolytic virus (OV), T-Vec (an engineered herpes virus), in clinical trials with breast cancer. The combination treatment increased $CD8^+$ T cells and heightened the PD-L1 protein expression level. Based on the success of the trial utilizing OVs as an immunotherapy treatment, the potential to treat other more difficult cancer types with a virus is promising [4].

1.3 The Promise of Oncolytic Viruses in Immunotherapy

One approach to exploit the immune system for cancer immunotherapies is to introduce a OV to the tumor. Infection of the tumor by an OV has the potential to induce immune infiltration to change the TME. Both the innate and adaptive immune systems are involved in cancer cell immunosurveillance and destruction [5]. Changes in the TME of a solid tumor by an OV can enhance the anti-tumor immunity and release neoantigens. Efficacy enhancements were observed with the introduction of OVs in *in vitro* breast cancer studies. Cell viability, after 36 hours of wild type vesicular stomatitis virus (wt VSV) infection, showed a decrease across several breast cancer cell lines. The enhancements in the study demonstrate how the use of an OV has the propensity to be a success option for treatment. The mechanism for introducing OVs to a TME causes significant changes [5]. Infiltrating the TME causes changes that can alter the progression of the tumor, since the condition of its microenvironment is key for its cell growth success. Despite the clinical success some cases have experienced with reduction in tumor size and ceased metastasis, ‘cold cancers’ remains resistant to a wide range of infections. By introducing

a protein that induces adequate apoptosis with the OV, ‘cold cancers’ can dynamically be changed to ‘hot cancers’ for successful immunotherapy treatment [6].

1.3.1 Benefits of Engineering VSV with Smac Protein

In a study using an EMT6 breast carcinoma model, wt VSV infection induced cytokine and chemokine secretion which promoted $CD8^+$ T cell tumor infiltration. The combination of the OV with a Smac mimetic, LCL161, reinvigorated the exhausted $CD8^+$ T cells and polarized the tumor-associated macrophages (TAM) to the M1- like macrophages, which initiate immune response[6]. The results of the oncolytic VSV infection to the EMT6 tumor suggest that the effects could be enhanced if the microenvironment of the tumor is altered. Hence, a transgene encoding Smac was inserted directly into the genome of VSV.

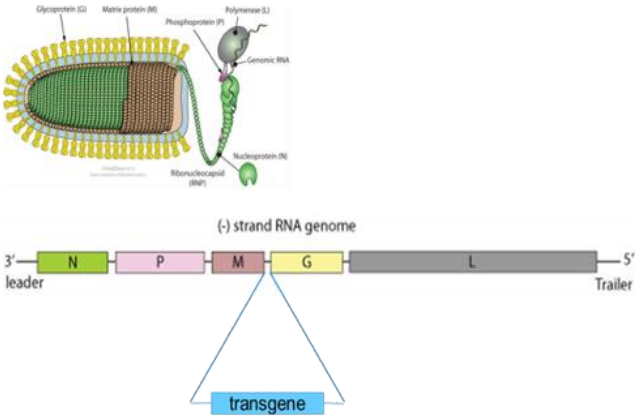

Figure 1.2: VSV and the insertion of a transgene between M and G nucleoproteins in the negative strand RNA genome.

VSV is a negative RNA strand virus that has a broad cellular tropism. The receptor for VSV is the low- density lipoprotein (LDL) and its homologs, which renders VSV’s ability to infect a wide range of cells. The genome of VSV (Figure 1.2) is a single-strand RNA enwrapped in the nucleocapsid. From the 3^0 end, there are five viral-encoded genes: N, P, M, G, and L representing nucleocapsid, phosphoprotein, matrix, glycoprotein, and the L protein. The level of

mRNA transcription decreases from N to L, with about 30% reduction compared to the preceding gene [7].

The products of N, P, and M are required to be expressed proportionally for efficient viral replication and assembly. So, the Smac transgene was inserted between M and G to allow for expression after the viral replication was established. The multi-cycle growth curve of VSV-S was compared to that of wt VSV. The final titer of VSV-S was similar to that of wt VSV, but its growth rate was a little higher in the initial stage of infection. The average plaque size of VSV-S infection was larger than that of wt VSV, which indicates that insertion of the Smac gene in VSV genome between M and G did not compromise VSV growth in cell culture [7].

VSV-S, as a viral vector for Smac expression in tumor cells to induce adequate apoptosis, is effective [8]. The second mitochondria-derived activator of caspase (SMAC) is a protein associated with the mitochondrial outer membrane. Smac plays a key role in apoptosis pathways by interacting with the inhibitor of apoptosis proteins (IAPs). During apoptotic stress, Smac in the outer membrane of the mitochondria is released into the cytosol and mitigates the activities of IAPs: cIAP1, cIAP2, XIAP, survivin, NAIP, ML-IAP and BRUCE. Once released by the mitochondria, Smac interacts with various IAPs to release their inhibition of the intrinsic apoptotic pathway by allowing caspase-9 and caspase-3 to be activated, shown in Figure 1.3 [9]. Smac mimetics (SMs) enhance apoptosis in a large number of difficult cancer cell lines. Thus, its expression in VSV has the potential to change the TME to be more immunologically active.

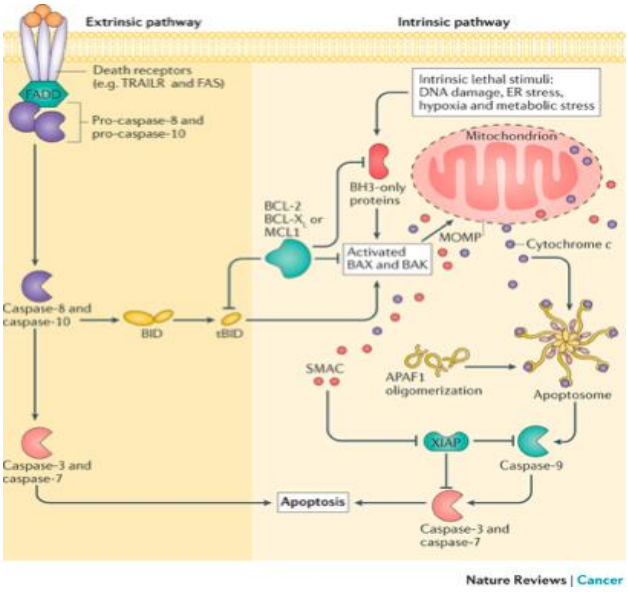

Figure 1.3 Intrinsic and extrinsic pathway of apoptosis

SMs can sensitize tumor cells to OVs and can greatly enhance the antitumor effects when engineered together. In recent studies, the combination of Smac mimetic and an OV resulted in synergistic enhancement for the infiltration of $CD8^+$ T cells in immunosuppressed tumors [10].

Delivering Smac to the tumor cell by a viral vector, VSV, has the advantage to replicate and spread in tumor cells to express at high levels. The pharmaceutical agent can offset the upregulated expression of IAPs in tumor cells while the proteins biological functions remain consistent in comparison to being recapitulated in SMs. SMs are substrates of p-glycoprotein whom are subject to efflux via the multidrug resistance mechanism [11]. By encoding Smac into the genome of VSV, efflux by the p-glycoprotein can be eliminate as a concern. Moreover, the infection by VSV itself will trigger apoptosis, which will be synergetic with the antitumor activity of Smac. The armed OV has the potential to alter the TME more effectively in comparison with its wildtype counterpart. The ability of Smac to interact with IAPs makes VSV-S more effective in killing cancer cells. This generation of VSV-S was constructed via reverse genetics, as stated

previously. The transgene of Smac was cloned in the VSV genome in the cDNA vector. Lipofectamine (Thermo Fisher Scientific) co-transfection of the VSV-S cDNA with plasmid-N (pN), plasmid-P (pP), and plasmid-L (pL) into BSR cells infected with vaccinia virus expressing T7 RNA polymerase, vTF7-3, rescued VSV-S. Vectors pN, pP, and pL express the nucleocapsid, phosphoprotein, and the L protein, respectively [12]. The rescue of wt VSV by reverse genetics was also made possible by using the wild-type (WT) genomic cDNA.

2 EXPERIMENTATION

2.1 Adaptation of Murine KPC to VSV-S by Limited Dilution

To strengthen the infectivity targeting PDAC cells, the virus was adapted via limited dilution. VSV-S was adapted to a pancreatic cancer cell line, KPC, that was derived from the $Kras^{G12D}$; $Trp53^{R172H}$; Pdx1-Cre (KPC) mouse model. Adaptation allows the virus to evolve through a series of passages either in cell culture or in an animal host [12]. A stock of VSV-S was prepped by infecting HeLa cells, a cervical cancer cell line.

In the infected HeLa cell culture medium, the titer of VSV-S was $1.5\pm0.15x10^6$ PFU/mL, outlined in Table 2.1. A set of VSV-S inocula was prepared by 10-fold serial dilution (10^{-1} to 10^{-6}). The virus inocula was added to different wells of KPC cells; the strategy is shown in Figure 2.1. The same method was also carried out with a wt VSV that expresses a viral P protein fused with mCherry. In the next passage, the virus inoculum is picked from the infected well that has been inoculated with the lowest dilution of virus samples, judged by the same cytopathogenic effect (CPE) as cells infected with fluorescent wt VSV. After 5 passages, the adapted VSV-S is plaque purified twice and is labeled as VSV-S_{KPC}. The titers of VSV-S_{KPC} are determined by plaque assays (PFU) in HeLa cells, and TCID50 in KPC cells in triplets. In adaptation of VSV-S

to KPC, 3 passages are necessary to reach the high limit, and then 2 more passages were carried out. A comparison of VSV-S_{KPC} versus VSV-S titers are summarized in Table 2.1. Based on the data, the adaptation by limited dilution increased the infectivity of VSV-S in KPC cells by 20-fold. The cytopathogenic effect (CPE) was examined under a microscope 24 hour post-infection. The dilution at which KPC cells were effectively infected by VSV-S was selected based on the level of CPE that was the same for the fluorescent wt VSV.

Table 2.1: Titers of Adapted VSV-S

	VSV-S_{KPC}	VSV-S
PFU/mL (HeLa)	$3.3\pm0.7x10^7$	$1.5\pm0.15x10^6$
TCID50 (KPC)	$6.3\pm1.1x10^7$	$3.4\pm0.6x10^6$

Evolutionary mutations in the serial passages occur, causing the newly emerged virus to prefer infection in the specific cell; which is a remarkable capability of the OV.

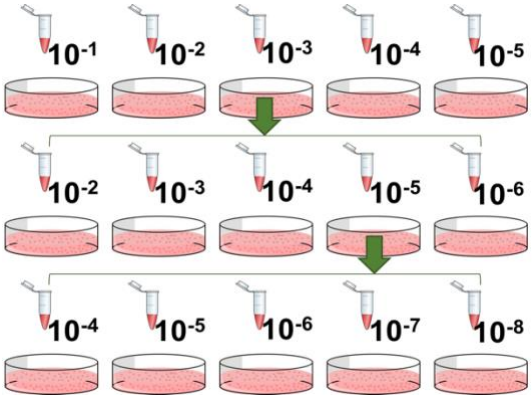

Figure 2.1 Demonstration of Adaptation by Limited Dilution

To demonstrate the adapted OVs ability to treat the difficult tumor in succession, *in vivo* studies were conducted. Tumor treatment included intratumorally injections of VSV-S_{KPC} several days after subcutaneous implantation of 0.5×10^6 KPC_luc cells on the left flank. The tumors were injected in both male and female C57BL/6 models. Since VSV- S_{KPC} has an increased infectivity of KPC cells, the virus was propagated in KPC cells prior to infection.

2.2 Growth and Concentration of VSV-S_{KPC}

The pancreatic cancer cell line of interest, KPC, was cultured and infected with VSV-S for the study using the C57BL/6 model. KPC cells were grown in DMEM with penicillin and streptomycin, supplemented with 10% fetal bovine serum (FBS). Cells were split onto several 150 mm in diameter plates and incubated until they grew to confluence. After approximately 24 hours, the culture media was removed via suction and the cells were washed once with warm Dulbecco's phosphate-buffered saline (DPBS) to remove the old media. To infect the cells with VSV-S, 1 mL of $DMEM^{++PS}$ absent of FBS was added to each plate along with 100 uL of the engineered OV. Cells were infected at MOI =0.1. The cells were incubated for an hour with constant rotation, to ensure all cells were infected. An additional 12 mL of media was added to the plates and the infected cells were harvested for 24-48 hours.

The supernatants from infected cells were clarified and then concentrated into pellets via ultracentrifugation (Beckman Coulter). After clarification at low speed centrifugation, the centrifugation tubes containing the cleared supernatant were allowed to spin at 16100 RPM at 4 °C for 2 ½ hours using a 45 Ti fixed-angle titanium rotor. The media was discarded and the pellets were then resuspended with 5% sucrose in phosphate buffer solution PBS, stirred and pipetted into an 1 mL cryptogenic tube with a total volume of 0.5 mL. Several cryptogenic tubes were collected and stored in liquid nitrogen for later use.

2.3 Plaque Assay and Calculation of Titers

Calculating the plaque forming units, data shown in Table 2.1, was essential for counting the numbers of viruses present in the selected dilution. In the table, data comparisons between the wildtype VSV and the adapted virus is shown for plaque assay and TCID50 calculation.

Overall, the titer for the adapted VSV was higher than its predecessor. Thus, the selective infectivity was increased.

To preform plaque assay, serial dilutions of the virus stock were completed using a similar strategy to Figure 2.1. Wells of monolayer KPC cells were infected with 0.5 mL of virus inoculum, incubated for 1 h at 37 °C, 5% CO_2, and a layer of 0.8% Seaplaque agarose, a nutrient-rich medium, was added to each well. The plate was incubated for 48 h at 37 °C, 5% CO_2, after the gel was allowed to form in each well. The infected cells released a viral progeny. The gel prohibited the spread of the virus and resulted in a plaque, which is a circular virus zone. A dye was then utilized to develop contrast between the living cells and the plaques. The well with a significant amount of plaques, between 10 – 100 were counted exactly. Based on the virus stock dilution used, 10^{-1}-10^{-7}, the dilution was multiplied by the volume of virus added to the well and the number of plaques were divided by that product. The equation: $\frac{PFU}{mL} = \frac{average\ of\ PFU}{(dilution)(volume\ of\ diluted\ virus\ added\ to\ well)}$ was used for the plaque assay calculation for KPC adapted VSV-S and its wildtype, which are shown in Table 2.1.

3 RESULTS

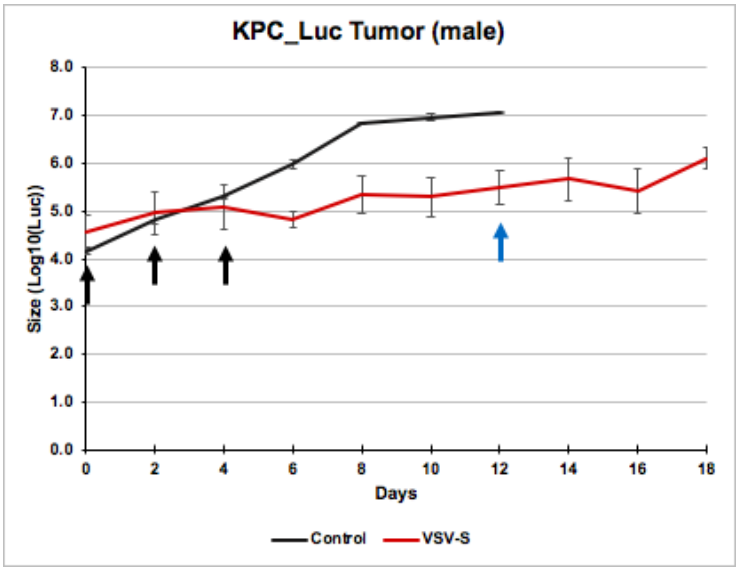

Figure 3.1: Size of KPC_luc Tumor in C57BL/6 Male Models with Black Line Representing the Control Mice and Red Line Representing Treated Mice. Blue Arrow Represents Days of Injection of Anti-PD-1 and Black Arrows Represent Injection of VSV-S_{KPC}

The C57BL/6 male mice were injected with $0.5x10^6$ KPC_Luc cells subcutaneously on the left flank. The size of tumors was monitored by luciferase activities using an IVIS imager. On Days 0, 2 and 4, indicated by the black arrows, $3.0x10^7$ PFU of KPC adapted VSV-S was intratumorally injected in each mouse. On Day 12, indicated by the blue arrow, 40 µg of mouse anti-PD-1 (BioXcell) was intratumorally injected in each mouse. The red line on the figure represents the average of the five mice. Intratumorally injection of phosphate buffer solution PBS was carried out in two control mice also indicated by the black arrows (Figure 3.1).

Similarly, the C57BL/6 female mice were injected with $0.5x10^6$ KPC_Luc cells subcutaneously. The size of tumors was again monitored by luciferase activities using an IVIS imager. On Days 0, 2 and 4, indicated by the black arrows, $3.0x10^7$ PFU of KPC adapted VSV-S was intratumorally injected in each mouse. On Days 6 and 12, indicated by the blue arrows, 40 µg of mouse anti-PD-1 (BioXcell) was intratumorally injected in each mouse. Mice 1 and 2 were euthanized on Day 10 and 12, respectively. The red line represents the average of the three surviving mice (Figure 3.2). From the graph, its certain that the control mice tumors were able to

grow exponentially without the adapted VSV-S treatment. The tumor that received the treatment were able to experience complete regression. A remarkable achievement for the immunotherapy treatment. In comparison to the trajectory of the male tumors, it is clear that the female models work better with the treatment. The immune response variance between genders is an important factor to consider and examine.

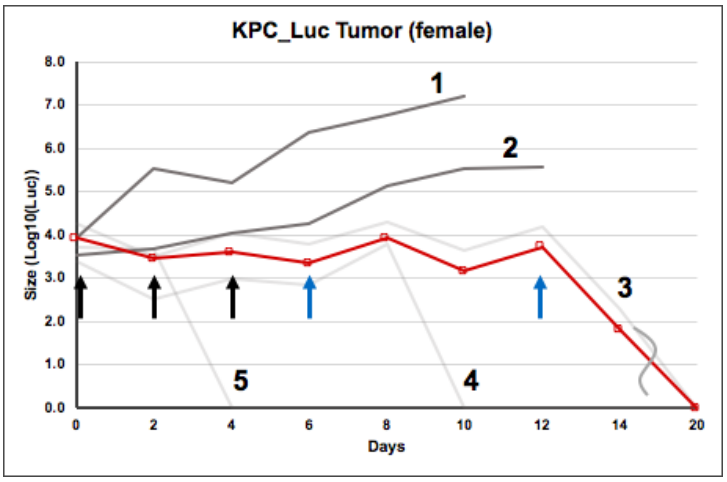

Figure 3.2: Size of Tumor in C57BL/6 Male Models; Black Line Representing the Control Mice and Red Line Representing Treated Mice. Blue Arrow Represents Days of Injection of Anti-PD-1 and Black Arrows Represent Injection of VSV-S_{KPC}

To directly confirm the selective infectivity, infection of KPC and MS1 cells by adapted VSV-S were compared by their CC_{50} values measured with MTT assays shown in Figure 3.3A. The selectivity is 94 -fold for KPC cells over MS1 cells. These results demonstrated that VSV-S adaptation by limited dilution is readily applicable to target cancer cells in a very short period of time, usually a few days [14]. To confirm that adaptation by limited dilution increases selective infection by VSV-S_{KPC}, mouse KPC and MS1 cells (pancreatic islet endothelial cell line, ATCC) were infected with VSV-S_{KPC} and wt VSV at different MOIs in Figure 3.3A. KPC cells could be effectively infected by wt VSV at MOI=0.1, and MS1 cells, at MOI=1. On the other hand, KPC cells could be effectively infected by VSV-S_{KPC} at MOI=0.01, and MS1 cells, at MOI=10. The

selective ratio is 10:1 (KPC:MS1) for wt VSV based on CC_{50} measured by MTT assays, whereas the selective ratio is 94:1 (KPC:MS1) for VSV-S_{KPC}. Based on this comparison, selective infection of VSV-S was increased by adaptation by limited infection.

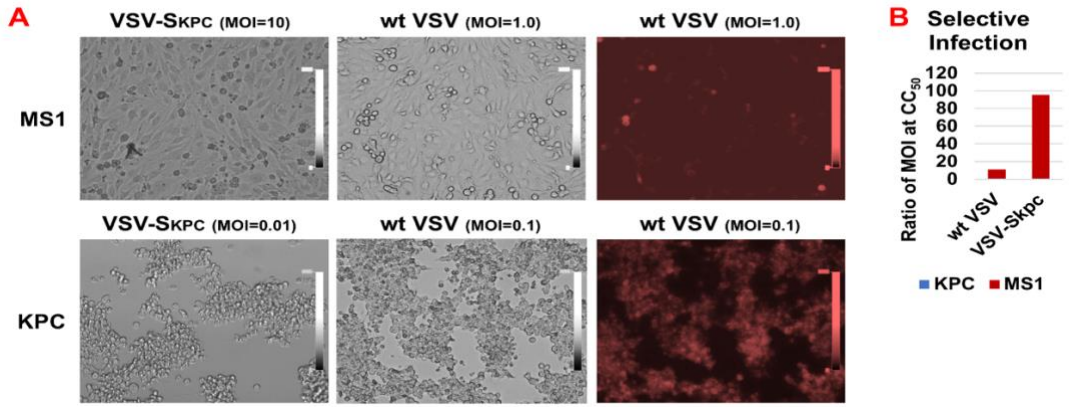

Figure 3.3: **A**. KPC and MS1 cells: pancreatic islet endothelial cell line ATCC, infected with VSV-S_{KPC} and wt VSV. MS1 infected with VSV-S_{KPC} at MOI=10, wt VSV at MOI=1.0 and KPC infected with VSV-S_{KPC} at MOI=0.01, wt VSV at MOI=0.1. B. Selective ratio is 10:1 (KPC:MS1) for wt VSV and 94:1 (KPC:MS1) for VSV-S_{KPC}.

3.1 TME Changes Induced by Adapted VSV-S

The KPC_luc tumor samples were collected on day 2 and 8, after the second injection of VSV-S or PBS control. Shown in Figure 3.4 and 3.5 the total amounts of leucocytes (CD45+) in tumor samples were increased by 3-3.5-fold with VSV-S treatment, compared to the control, after 8 days. Yet, the ratio between lymphocytes and myeloid cells, or CD8+ and CD4+ T cells, was not changed significantly despite that the total number of lymphocytes greatly increased. Mainly, changes in the myeloid cells largely increased neutrophil populations, and decreased macrophages, which was obvious just 2 days after VSV-S treatment, with the decrease of macrophages being more visible. Indicating that treatment with VSV-S caused strong inflammation in the tumors and largely increased tumor infiltrating lymphocytes (TIL) [15].

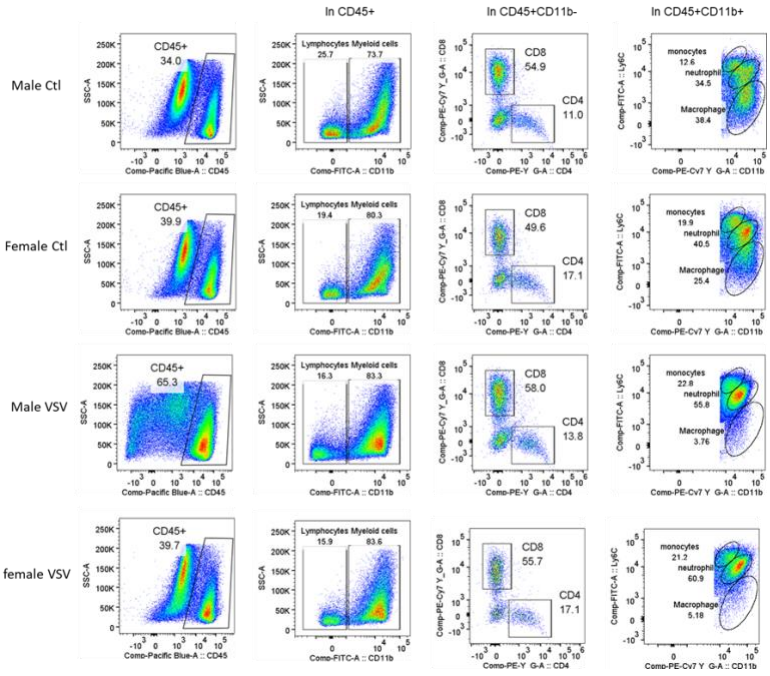

Figure 3.4: Tumor microenvironment (TME) analysis. (i) Flow cytometry of isolated male and female tumor cells after 2 days of treatment with intratumoral injection of VSV-S or control PBS. Gates and biomarkers are labelled.

The populations of M2 versus M1 macrophages were compared during a large reduction in macrophage population to access the immunosuppressive TME regression. Significant reductions of M2 macrophages ($CD206^+$) were observed just 8 days after VSV-S treatment, with significant reductions 2 days after VSV-S treatment. The populations of M1 macrophages ($CD86^+$) were also reduced, which is potentially the result of significant reductions in the total number of macrophages. In all, these observations suggest that the VSV-S treatment could alter the immunosuppressive TME.

The large increase of neutrophils in tumors could cause more death of cancer cells due to innate immunity [16]. Several studies confirmed that neutrophils participate in tumor cell clearance upon OV infection of tumors [16-18], which is also consistent with the results of efficacious tumor regression by VSV-S treatment of breast cancer xenografts [3].

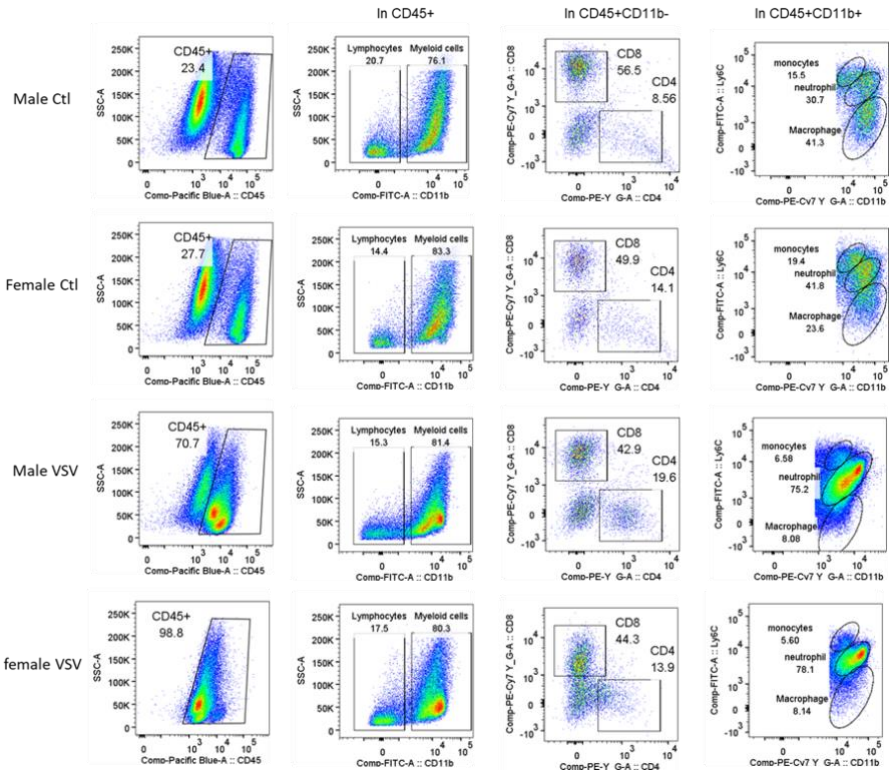

Figure 3.5: Tumor microenvironment (TME) analysis. (i) Flow cytometry of isolated male and female tumor cells after 8 days of treatment with intratumoral injection of VSV-S or control PBS. Gates and biomarkers are labelled.

More importantly, treatment with an OV altered the TME which in turn enhanced the efficacy of this immunotherapy treatment. This advantage is illustrated by more than 3-fold changes of leucocytes in the tumors infected by VSV-S. The change was noticeable after day 2, and more obvious after 8 days, during the final VSV-S infection. Even though the total number of lymphocytes was greatly increased, the ratio between lymphocytes and myeloid cells, or between $CD8^+$ and $CD4^+$ T cells, however, was not changed significantly.

The most important changes of myeloid cells are the dramatic increase of neutrophils, and the decrease of macrophages. These changes are consistent with strong inflammation in the tumor caused by VSV-S infection. Neutrophils exhibit tumor suppressive activities by generating reactive oxygen species (ROS), activation of the IFN-γ pathway, and up-regulation of antigen presentation [16]. The immunosuppressive TME was most likely reverted by the large reduction

of M2-like macrophages. Based on the date summarized in Figures 3.1 and 3.2, it is clear that treatment with VSV-S caused strong inflammation in the tumors and largely increased tumor infiltrating lymphocytes (TIL) [17].

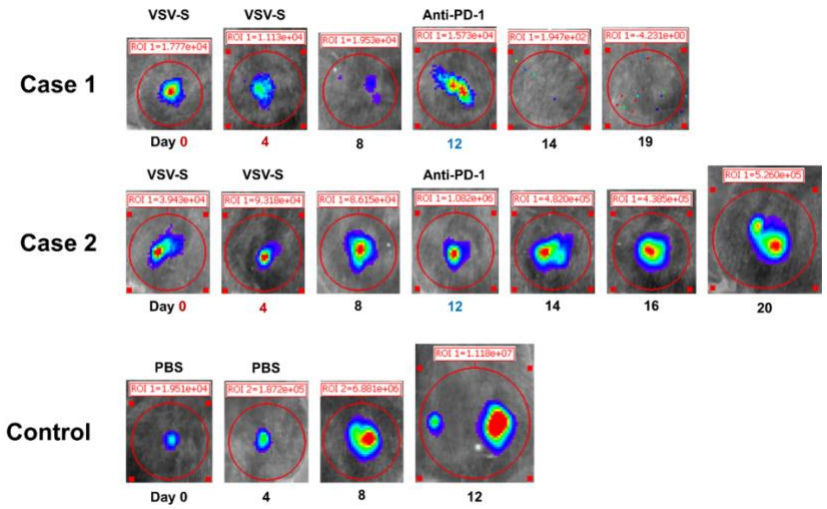

Figure 3.6: C57BL/6 Female Tumor by Luciferin on the Initial day of Injection of VSV-S_{KPC}, Day 7 and Day 19

After subcutaneous implantation of KPC-luc cells, the tumors were monitored with IVIS imagining. When tumors became visible, the size was measured as the integrated luciferase activity detailed in Figure 3.6. On Days 0, 2, and 4, $3.0X10^7$ PFU of VSV-S_{KPC} in 30 µL was intratumorally injected in each mouse, and tumor growth was recorded every 2 days till Day 22. The controls used 30 µL of PBS and intratumorally injected it into the tumor on the same days. On Day 12, 40 µg of anti-PD-1 antibody was intratumorally injected in each of the VSV-S_{KPC} treated mice. The quantitation was determined to be $4.5x10^6$ U/g of tumor mass.

VSV-S treatment was able to inhibit the tumor growth rate in comparison to the control ($p<0.0006$). Mostly, VSV-S treatment effectively arrested tumor growth. With a followed-up treatment of anti-PD-1 antibody, the tumor was able to completely regress. Yet, complete

regression of the tumor was not achieved in some cases highlighted in Figure 3.6, case 2. However, obvious inhibition of tumor growth by VSV-S treatment was observed with a follow-up treatment of anti-PD-1 antibody. The best outcome for the combination treatment with VSV-S and anti-PD-1 antibody, was the survival of the tumor bearing mice was increased. The median time to death (MTD) was doubled to >27.4 days in comparison to MTD of 14.9 days for the control group. There was also interesting differences in tumor growth were found between female and male mice, (Figure 3.1 and Figure 3.2) which sparked interest in the immune response variance between the sexes. The tumor growth rate is faster in male than in female mice, with or without treatment with VSV-S.

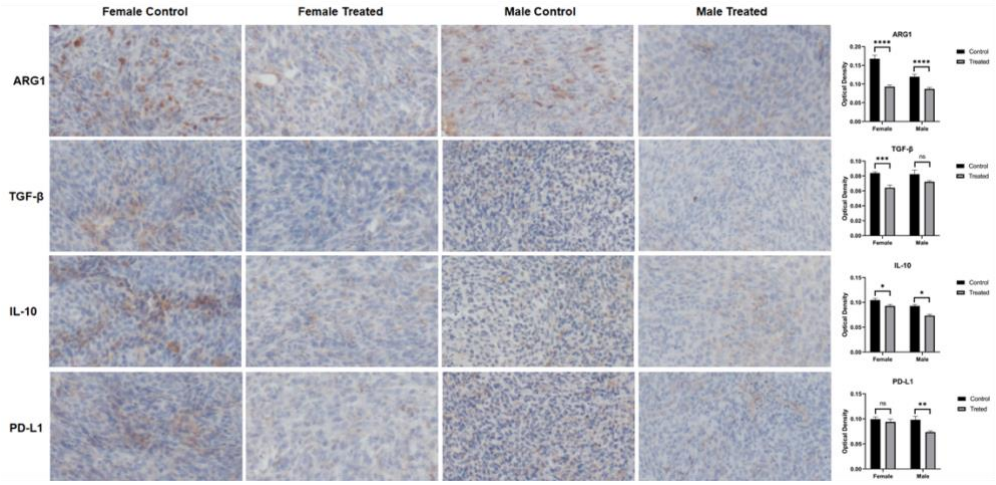

Figure 3.7: IHC Staining Results For PDAC of Cytokine IL-10 Expression in C57Bl/6 Model, A. Female 10 days; B. Female 20 days; C. Female treated 10 days; D. Female treated 20 days; E. Male 10 days; F. Male 20 days; G. Male treated 10 days; H. Male treated 20 days.

The large increase of neutrophils in tumors could cause more death of cancer cells due to innate immunity [18]. Several studies confirmed that neutrophils participated in tumor cell clearance upon OV infection of tumors[19-22], which is also consistent with our previous results of efficacious tumor regression by VSV-S treatment of breast cancer xenografts [22].

3.2 Immunohistochemistry Results

The changes to the TME due to VSV-S treatment are examined in depth using immunohistochemistry staining of the paraffin-embedded tumor tissues. Immunosuppressive factors argenase1 (ARG1), interleukin 10 (IL-10), and transforming growth factor-beta (TGF-β) were significantly decreased in both male and female mice, which indicates that the VSV-S treatment could reduce the immunosuppressive effect in the TME (Figure 3.7). The PD-L1 expression level also decreased after the treatment, shown in Figure 3.7. Typically, the expression of PD-L1 increases in the tumor to down-regulate the ongoing immune activation. This mechanism allows the expression of PD-L1 on tumor cells to inhibit local anti-tumor T cell responses [15]. However, the increased expression of tumor PD-L1 was mostly in myeloid cells [16]. The observed decrease of PD-L1 expression after VSV-S treatment may be associated with changes in myeloid cells.

The considerable reduction of macrophages, especially M2-like macrophages, most likely were related to reverting the immunosuppressive TME. To confirm this notion, levels of arginase 1 (ARG1), TGF-, and IL-10 in KPC tumors were analyzed by immunohistochemistry before and after treatment, shown in Figure 3.7. It was observed that the optical density of the treated tumors, shown in gray, had decreased levels of arginase 1, TGF- β, PD-L-1, and IL-10. This indicates that the TME is altered with the infection of adapted VSV-S. Cells associated with vital immunosuppressive functions are known as myeloid-derived suppressor cells (MDSCs), which express arginase. Arginase plays an opposite role in immune response and is one of the primary mechanisms of immunosuppression [22], so a decrease in its levels is desired. MDSCs also express suppressive cytokines like TGF-β and IL-10 in the tumor. The changes made in the immunosuppressive TME by VSV-S infection of the tumor reveal a correlation. The observed

reduction in PD-L1 may be associated with its decline in myeloid cells, not necessarily PD-L1 expressed in tumor cells. Extended regression of tumors can be achieved by combination regimens of OV treatment and immunotherapy.

4 DISCUSSION

4.1 Evaluate antitumor applications of VSV-S_{KPC} in the syngeneic model for pancreatic cancer

Tumor-associated macrophages (TAM) play an essential role in the processes of tumor carcinogenesis, including the escape of cancer cells from the tumor into the circulation and the suppression of antitumor immune functions and drug resistance. Univariate analysis showed that worse overall patient survival was significantly associated with high CD59 expression in the tumor tissues. Therefore, overexpression of CD59 may be a biomarker indicating worse survival for pancreatic cancer patients. The data suggest that CD59 expression is proportional to the TAM infiltration in pancreatic cancer tissues. There is likely cross-talk and cooperation between TAMs and CD59 expression in pancreatic cancer cells [20].

The ultimate application of VSV-S or its derivatives is to enhance treatment efficacy for PDAC and other cancers. As mentioned previously, KPC tumors were implanted under the skin of both male and female C57BL/6 models. The adapted VSV-S was used as treatment with the combination of anti-PD-1. It was determined from the study that treatment with the anti-PD-1 antibody, after 8 days of the virus injection, prolonged inhibition of tumor growth and even helped to eliminate the tumor in the female models (3 out of 8 female mice, and 2 out of 8 male mice). As previously reported, anti-PD-1 antibodies alone cannot change the tumor growth or survival in KPC mouse models. Combination therapies only increased survival. The delayed administration of the immune checkpoint inhibitor combined with the OV is consistent with the

temporal change of the TME [25]. The combination therapy significantly extended the survival of tumor-bearing mice.

4.2 Immune Response Variance Between Male and Female Models

There are two observations in the study that are fascinating. First, the growth rate of tumors in female mice after treatment was significantly slower than in male mice. The responses are also more favorable in female mice versus male mice. This observation was consistent with patient incident case numbers, and deaths which peaked at the ages of 65–69 years for males and 75–79 years for females [25]. PDAC appears to be more lethal to males in comparison to females. Data suggests that female patients may respond better to immunotherapy and have a better chance of survival. Secondly, the efficacy of the treatment with the OV appeared to be dependent on the initial tumor size when treatment began. This dependence is due to the degree of virus spread within the tumor mass. When the tumor size is smaller, it is expected that a higher portion of the mass is directly exposed to the infection upon injection. Tumor growth in the male models was reportedly faster than the females. To study cell-cell interaction in the TME, spatial information at the resolution of a single cell is essential, and a microscopy is the most helpful tool to obtain

it.

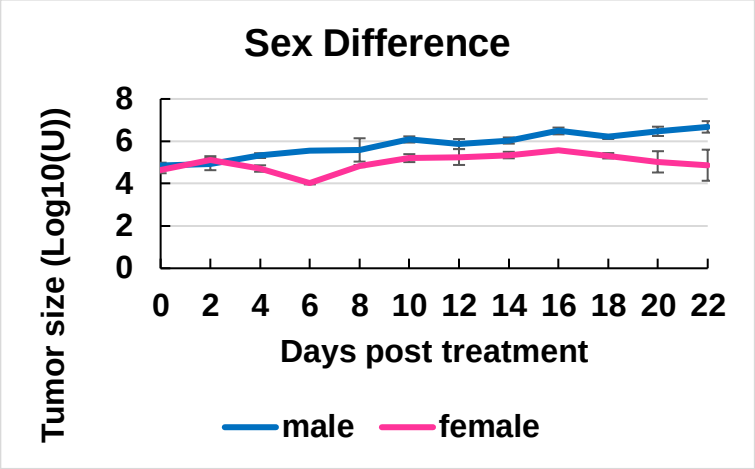

Figure 4.1: The tumor growth curves of treated female mice (n=3) (pink) and male mice (n=3) (blue) groups. Tumor size was presented as logarithm values of the luciferase activity measured on an IVIS imager. Error bars represent the standard deviations. Treatment regimen was intratumoral injection of 3.0 x10^7 PFU of VSV-S_{KPC} on Days 0, 2 and 4, and 40 µg of anti-PD-1 antibody on Day 12.

The immune response variation between sexes has notable differences. Females are parasitized less often than men, with male immune systems having a lesser ability to fight off pathogens. Females usually have a more robust immune response, which is not always positive. Often this makes them more susceptible to immunopathology such as autoimmunity compared to males. This susceptibility to autoimmune disease has been associated with immune response components such as particular gene variants at the major histocompatibility complex (MHC). MHC was central to the adaptive immune response; a set of highly polymorphic genes encodes these molecules. High diversity of MHC gene variants has been theorized to be beneficial; this may be due to the ability to recognize a broader range of pathogens or the increased chance of carrying advantageous genes that maximize disease resistance [18].

5 CONCLUSION/ SIGNIFCANCE

Immunotherapy treatment for PDAC using oncolytic viruses and immune checkpoint inhibitors is a promising approach. However, many challenges remain within the method as some tumors are resistant to infection and fail to respond to the inhibitors adequately. The efficacy of VSV-S was enhanced in previous *in vivo* studies, with several breast cancer cell lines, compared to its wildtype counterpart. Infection was more extensive by VSV-S, especially for the T-47D cell line, which expresses very high levels of XIAP. To summarize the results from the infection of PDAC, adaption of the virus and increasing infectivity allow treatment to overcome the obstacles mentioned.

The activation of caspase-9 and caspase-3 from the intrinsic pathway of apoptosis resulted from the infection of VSV-S. The activation was made possible by inserting a transgene-like Smac in the genome of VSV. The study with PDAC demonstrated the effectivity of VSV-S with a immunologically ‘cold cancer’. Pancreatic ductal adenocarcinoma has shown therapy resistance with other therapy methods but adapted VSV-S can overcome this difficulty. In cases with the female models, the KPC tumors experienced a complete regression which is an impressive result for this specific cancer cell line. The overall significance of the PDAC study demonstrated how the efficacy of VSV-S was enhanced by adaption to the cancer cell line. Moreover, by increasing the infectivity of the OV to its target tumor, regression or complete inhibition of the tumor is possible.

The use of an armed OV suggests that improvements in immunotherapy treatments for PDAC are achievable. The methods discussed can turn the disease from immunologically “cold” to immunologically “hot.” The therapy by immune checkpoint blockade was especially promising. Treatment with VSV-S has advantages over other immunotherapy treatment options.

VSV has a high mutation rate, and the virus can be adapted to the specific cell line to increase infectivity considerably (e.g., 20-fold in mouse KPC cells). Using an OV, infection of tumor cells can initiate inflammatory responses in the TME and release many tumor antigens to evoke anti-tumor immunity.

Combining treatments with chemotherapy medication and immunotherapy is tolerable but not overly conclusive as a viable option. From the IHC staining, a change in the TME was observed. A decrease in the optical density of several markers, which contribute to the suppressive TME of PDAC, was witnessed. In the infected tumors, neutrophils were significantly increased, whereas macrophages were primarily reduced, especially immunosuppressive M2 macrophages. These changes are consistent with strong inflammation in the tumor caused by VSV-S infection. The overall TME was also more immunologically active, proven by the reduced levels of cytokines and biomarkers, including TGF-β, Arginase -1, and IL-10. To conclude, VSV-S successfully activated the immunosuppressive TME and inhibited tumor growth in pancreatic cancer.

REFERENCES

1. Sarantis, P., Koustas, E., Papadimitropoulou, A., Papavassiliou, A. G., and Karamouzis, M. V. 2020, *Pancreatic ductal adenocarcinoma: Treatment hurdles, tumor microenvironment and immunotherapy*.
2. Ohtani, H. "Stromal reaction in cancer tissue: pathophysiologic significance of the expression of matrix-degrading enzymes in relation to matrix turnover and immune/inflammatory reactions." *Pathology international* vol. 48,1 (1998): 1-9. doi:10.1111/j.1440-1827.1998.tb03820.x
3. Types of Pancreatic Cancer. *Pancreatic Cancer Action Network.* PanCAN, PanCAN's Scientific and Medical Advisory Board, University of Pennsylvania, Memorial Sloan-Kettering Cancer Center, Virginia Mason Medical Center. 2020, October 23
4. Zeltz, Cédric et al. "Cancer-associated fibroblasts in desmoplastic tumors: emerging role of integrins." *Seminars in cancer biology* vol. 62 (2020): 166-181. doi:10.1016/j.semcancer.2019.08.004
5. *Gemcitabine for Patients with Advanced Pancreatic Adenocarcinoma.* Cancers (Basel), 2018. **10**(6). Hajda, J., et al., *A non-controlled, single arm, open label, phase II study of intravenous and intratumoral administration of ParvOryx in patients with metastatic, inoperable pancreatic cancer: ParvOryx02 protocol.* BMC Cancer, 2017. **17**(1): p. 576.
6. Sarantis, Panagiotis et al. "Pancreatic ductal adenocarcinoma: Treatment hurdles, tumor microenvironment and immunotherapy." *World journal of gastrointestinal oncology* vol. 12,2 (2020): 173-181. doi:10.4251/wjgo.v12.i2.173
7. Sitek, B., Bracht, T., Ahrens , M., Padden, J., Kalsch , J., Bertram, S., Megger, D. A., Eisenacher, M., Kocabayoglu, P., Meyer, H. E., Sipos , B., and Baba, H. A. Immunohistochemical Markers Distinguishing Cholangiocellular Carcinoma (CCC) from Pancreatic Ductal Adenocarcinoma (PDAC) Discovered by Proteomic Analysis of Microdissected Cells. *Molecular and Cellular Proteomics* . American Society for Biochemistry and Molecular Biology. 2016 Mar; **15**(3): 1072–1082
8. Elbanna, K.Y., Jang, HJ. & Kim, T.K. Imaging diagnosis and staging of pancreatic ductal adenocarcinoma: a comprehensive review. *Insights Imaging* **11,** 58 (2020). https://doi.org/10.1186/s13244-020-00861-y
9. Zainab, Heena et al. "Stromal desmoplasia as a possible prognostic indicator in different grades of oral squamous cell carcinoma." *Journal of oral and maxillofacial pathology : JOMFP* vol. 23,3 (2019): 338-343. doi:10.4103/jomfp.JOMFP_136_19
10. Bonaventura, Paola et al. "Cold Tumors: A Therapeutic Challenge for Immunotherapy." *Frontiers in immunology* vol. 10 168. 8 Feb. 2019, doi:10.3389/fimmu.2019.00168
11. Li, Ming O., Yisong Y. Wan, Shomyseh Sanjabi, Anna-Karin L. Robertson, and Richard A. Flavell. "Transforming Growth Factor-beta Regulation of Immune Responses." *Annual Review of Immunology*. U.S. National Library of Medicine. Web. 01 Apr. 2021.
12. Potter, Michelle. "Anti-PD-1: A Novel Immunotherapy." *Johns Hopkins Kimmel Cancer Center*. 18 July 2017. Web. 01 Apr. 2021.
13. Sarantis, Panagiotis, Evangelos Koustas, Adriana Papadimitropoulou, Athanasios G Papavassiliou, and Michalis V Karamouzis. "Pancreatic Ductal Adenocarcinoma: Treatment Hurdles, Tumor Microenvironment and Immunotherapy." 15 Feb. 2020. Web. 31 Mar. 2021.

14. Upadhrasta, Sireesha, and Lei Zheng. "Strategies in Developing Immunotherapy for Pancreatic Cancer: Recognizing and Correcting Multiple Immune "Defects" in the Tumor Microenvironment." *Journal of Clinical Medicine*. MDPI, 16 Sept. 2019. Web. 01 Apr. 2021.
15. Li MO, Wan YY, Sanjabi S, Robertson AK, Flavell RA. Transforming growth factor-beta regulation of immune responses. Annu Rev Immunol. 2006;24:99-146. doi: 10.1146/annurev.immunol.24.021605.090737. PMID: 16551245.
16. Blank C, Mackensen A (May 2007). "Contribution of the PD-L1/PD-1 pathway to T-cell exhaustion: an update on implications for chronic infections and tumor evasion". *Cancer Immunology, Immunotherapy*. **56** (5): 739–45.
17. Karwacz K, Bricogne C, MacDonald D, Arce F, Bennett CL, Collins M, Escors D (October 2011). "PD-L1 co-stimulation contributes to ligand-induced T cell receptor down-modulation on CD8+ T cells". *EMBO Molecular Medicine*. **3** (10): 581–92.
18. Agata Y, Kawasaki A, Nishimura H, Ishida Y, Tsubata T, Yagita H, Honjo T "Expression of the PD-1 antigen on the surface of stimulated mouse T and B lymphocytes". *International Immunology*. 8 (May 1996).(**5**): 765–72.
19. Yamazaki T, Akiba H, Iwai H, Matsuda H, Aoki M, Tanno Y, Shin T, Tsuchiya H, Pardoll DM, Okumura K, Azuma M, Yagita H "Expression of programmed death 1 ligands by murine T cells and APC". *Journal of Immunology*. **169** (November 2002).(10): 5538–45.
20. Balachandran VP: Dissecting the immune complexity of pancreatic cancer survivors through team science. AACR Virtual Special Conference: Pancreatic Cancer. Presented September 30, 2020.
21. IHC Tests (ImmunoHistoChemistry). *Breastcancer.org*. 2020, January 21
22. Kasper H. U., Drebber U., Dries V., and Dienes H. P. (2005) [Liver metastases: incidence and histogenesis]. *Z. Gastroenterol*. **43**, 1149–1157
23. Somoracz A., Tatrai P., Horvath G., Kiss A., Kupcsulik P., Kovalszky I., and Schaff Z. (2010) Agrin immunohistochemistry facilitates the determination of primary versus metastatic origin of liver carcinomas. *Hum. Pathol*. **41**, 1310–1319
24. *German S3-Guideline "S3-Leitlinie zum exokrinen Pankreaskarzinom" (2013) Version 1.0, AWMF registration number: 032/010OL*.
25. Borger D. R., Tanabe K. K., Fan K. C., Lopez H. U., Fantin V. R., Straley K. S., Schenkein D. P., Hezel A. F., Ancukiewicz M., Liebman H. M., Kwak E. L., Clark J. W., Ryan D. P., Deshpande V., Dias-Santagata D., Ellisen L. W., Zhu A. X., and Iafrate A. J. (2012) Frequent mutation of isocitrate dehydrogenase (IDH)1 and IDH2 in cholangiocarcinoma identified through broad-based tumor genotyping. *Oncologist* **17**, 72–79